

# Charge and orbital order in $\text{Fe}_3\text{O}_4$

I. Leonov<sup>1,2</sup>, A. N. Yaresko<sup>3</sup>, V. N. Antonov<sup>4</sup>, M. A. Korotin<sup>2</sup>, and V. I. Anisimov<sup>2</sup>

<sup>1</sup> *Theoretical Physics III, Institute for Physics, University of Augsburg, Germany*

<sup>2</sup> *Institute of Metal Physics, Russian Academy of Science-Ural Division, 620219 Yekaterinburg GSP-170, Russia*

<sup>3</sup> *Max-Planck Institute for the Physics of Complex Systems, Dresden, Germany and*

<sup>4</sup> *Institute of Metal Physics, Vernadskii Street, 03142 Kiev, Ukraine*

(Dated: June 27, 2018)

Charge and orbital ordering in the low-temperature monoclinic structure of magnetite ( $\text{Fe}_3\text{O}_4$ ) is investigated using LSDA+ $U$ . While the difference between  $t_{2g}$  minority occupancies of  $\text{Fe}_B^{2+}$  and  $\text{Fe}_B^{3+}$  cations is large and gives direct evidence for charge ordering, the screening is so effective that the total  $3d$  charge disproportion is rather small. The charge order has a pronounced [001] modulation, which is incompatible with the Anderson criterion. The orbital order agrees with the Kugel-Khomskii theory.

PACS numbers: 75.10.Jm, 75.30.Gw, 75.70.Ak

The magnetic properties of magnetite, the famous lodestone, has fascinated mankind for several thousand years already [1]. Even today, in view of the possible technological importance of this material for spintronics [2], and because of the still not well understood low-temperature properties, magnetite remains at the focus of active research.

Magnetite is a mixed-valent system and is the parent compound for magnetic materials such as maghemite ( $\text{Fe}_2\text{O}_3$ ) and spinel ferrites. At room temperature it crystallizes in the inverted cubic spinel structure  $Fd\bar{3}m$  with tetrahedral  $A$ -sites occupied by  $\text{Fe}^{3+}$  cations, whereas octahedral  $B$ -sites are occupied by an equal number of randomly distributed  $\text{Fe}^{2+}$  and  $\text{Fe}^{3+}$  cations. Magnetite is ferrimagnetic with an anomalous high critical temperature  $T_C \sim 860$  K, the  $A$ -site magnetic moments being aligned antiparallel to the  $B$ -site moments. At room temperature  $\text{Fe}_3\text{O}_4$  is a poor metal with an electronic conductivity of 4 m $\Omega$  cm. Upon further cooling a first-order metal-insulator (Verwey-) transition occurs at  $T_V \sim 120$  K where conductivity abruptly decreases by two orders of magnitude. According to Verwey this transition is caused by the ordering of  $\text{Fe}^{2+}$  cations on the  $B$  sublattice, with a simple charge arrangement of  $(001)_c$  planes (indexed on the cubic cell) alternately occupied by 2+ and 3+  $\text{Fe}_B$  cations (Verwey charge ordering model) [3, 4]. This particular charge order (CO) obeys the so-called Anderson criterion [5] for minimal electrostatic repulsion leading to a short range CO pattern, namely tetrahedra of  $B$ -sites with an equal number of 2+ and 3+ cations. Since then a wide range of other CO models has been proposed which, however, all make use of the Anderson criterion [6, 7].

Later experiments showed that the Verwey transition is accompanied by a structural distortion from cubic to the monoclinic structure which has not been fully resolved so far [7, 8]. Although the experiments rule out the Verwey CO below  $T_V$  all attempts to construct a refined CO model from neutron-scattering data set failed because neutron scattering is more sensitive to atomic

displacements than to charge ordering. In the absence of a definitive, experimentally determined structure many theoretical models for the low-temperature (LT) phase of magnetite [9] have been proposed. They include purely electronic [10, 11] and electron-phonon [12, 13] models for CO, as well as a bond dimerized ground state without charge separation [14]. In particular all previous LDA(+ $U$ ) calculations were performed for undistorted cubic unit cell. In spite of the fact that the amplitudes of these distortions are quite small this approximation for the LT unit cell in LSDA+ $U$  calculations results inevitably in the Verwey CO. This problem is overcome in our work using recently refined crystal structure [15, 16] in which the ground state with more complicated CO was found. This also confirms Szotek *et al.* [17] conclusion that the Verwey CO is not the ground state for magnetite, which is based on self-interaction corrected local spin density calculations for the refined LT crystal structure.

In this paper we report LSDA+ $U$  calculations [18, 19] in the tight-binding linear muffin-tin orbital (TBLMTO) calculation scheme for  $\text{Fe}_3\text{O}_4$  in the  $P2/c$  structure [15, 16]. Motivated by our results, we propose an order parameter, defined as the difference between  $t_{2g}$  minority spin occupancies of  $\text{Fe}_B^{2+}$  and  $\text{Fe}_B^{3+}$  cations. This order parameter is found to be quite large, although the total  $3d$  charge difference between these cations, is small. It seems certain that magnetite is long-range ordered below  $T_V$ , in contrast to the intermediate valence regime proposed by García *et al.* [20, 21, 22].

Recently, the LT superstructure of magnetite was refined by Wright *et al.* [15, 16]. The space group was confirmed to be monoclinic  $Cc$ , but the structure refinement was only possible in  $P2/c$  group. They proposed the  $a_c/\sqrt{2} \times a_c/\sqrt{2} \times 2a_c$  subcell ( $a_c$  is the cell parameter of the undistorted cubic unit cell) with  $P2/c$  space group symmetry. The additional  $Pmca$  orthorhombic symmetry constraints were also applied. The refined cell parameters were  $a = 5.94437(1)$  Å,  $b = 5.92471(2)$  Å,

$c = 16.77512(4)$  Å, and  $\beta = 90.236(1)^\circ$ . The structural evidence for the CO below the transition in the refined crystal structure, which is based on estimations of the mean  $B$ -site-to-oxygen distances or the bond valence sum (BVS) analyses, was also declared [15, 16]. However, this refined structure analysis has recently been found to be controversial [21]. The lack of atomic long-range order and, as a result, the intermediate valence regime below the Verwey transition were proposed. Indeed, a difference between averaged Fe-O distances of compressed and expanded FeO<sub>6</sub> octahedra corresponds to the maximum limit of charge disproportion ( $0.2\bar{e}$ ), which has the same order as the total sensitivity (including experimental errors) of BVS method. This contradiction as well as the ambiguity of proposed CO schemes (two different CO classes were proposed: class-I in the  $P2/c$  unit cell and class-II in the full  $Cc$  superstructure), is resolved in our electronic structure study.

We perform LSDA and LSDA+ $U$  calculations for Fe<sub>3</sub>O<sub>4</sub> in the  $P2/c$  structure. For simplicity we neglect the small spin-orbit coupling (in previous calculations for cubic Fe<sub>3</sub>O<sub>4</sub> spin-orbital splitting of the  $3d$ -band was found to be two orders of magnitude smaller than the crystal field splitting [23]). The LSDA calculations give only a half-metallic ferrimagnetic solution without CO. Partially filled bands at the Fermi level originate from the minority spin  $t_{2g}$  orbitals of Fe<sub>B</sub> cations. The tetrahedral Fe<sub>A</sub> cations do not participate in the formation of bands near the Fermi level, since their minority and majority spin  $3d$  states are completely occupied and completely empty, respectively. Thus, the LSDA results qualitatively agree with previous band-structure calculations for the cubic phase [17, 24, 25, 26]. Apparently, only crystal structure distortion from cubic to monoclinic phase is not sufficient to explain metal-insulator transition and charge ordering in magnetite. The electron-electron correlations, mainly in the  $3d$  shell of Fe cations, play significant role.

To proceed further we take into account the strong electronic correlations in Fe  $3d$  shell using LSDA+ $U$  method. In contrast to the LSDA, already with  $U$  and  $J$  obtained from constrained calculations (4.5 eV and 1 eV, respectively) a charge ordered insulator with energy gap of 0.03 eV was obtained. On the other hand, the calculation of  $U$  depends on theoretical approximations and, as a rule, the accuracy does not exceed 10-20%. A reasonably good agreement of the calculated gap of 0.18 eV with the experimental value of 0.14 eV [27] was found using the  $U$  value of 5 eV. As shown in Fig. 1, the gap opens between occupied and unoccupied  $t_{2g\downarrow}$  states of Fe<sub>B(1)}</sub><sup>2+</sup>, Fe<sub>B(4)}</sub><sup>2+</sup> and Fe<sub>B(2)}</sub><sup>3+</sup>, Fe<sub>B(3)}</sub><sup>3+</sup> respectively. The remaining unoccupied Fe<sub>B</sub> states are pushed by strong Coulomb repulsion to the energies above 2 eV.

The obtained CO is described by a dominant  $[001]_c$  charge density wave with a minor  $[00\frac{1}{2}]_c$  modulation in the phase of CO and coincides with the class-I CO, which

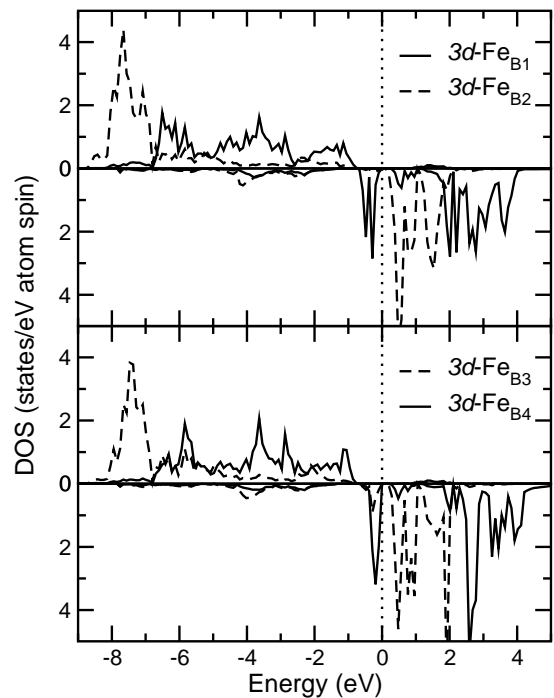


FIG. 1: Partial DOS obtained from the LSDA+ $U$  calculations with  $U=5$  eV and  $J=1$  eV for the low-temperature  $P2/c$  phase of Fe<sub>3</sub>O<sub>4</sub>. The top of the valence band is shown by dotted lines.

was proposed earlier by Wright *et al.* [15, 16]. Thus, the LSDA+ $U$  calculations confirm violation of the Anderson criterion for Fe<sub>3</sub>O<sub>4</sub> in the LT phase. In order to check the stability of the obtained CO solution we performed additional self-consistent LSDA+ $U$  calculations both for the  $P2/c$  structure and  $Cc$  supercell. In the first case the Verwey CO was used as the starting CO model, while in the second one we started from class-II CO, shown in Fig. 2 of Ref. 16. However, it was found that these CO models are unstable and the obtained self-consistent solutions coincide with the stable one found previously, i.e. for certain value of  $U$  the obtained CO does not depend on initial charge arrangement. Obviously, we did not check all possible CO scenarios within  $P2/c$  unit cell or  $Cc$  supercell, but our results consistently indicate that the obtained class-I CO solution is the ground state of Fe<sub>3</sub>O<sub>4</sub> in the LT phase. It is important to note that LSDA+ $U$  calculations performed for an undistorted  $P2/c$  supercell of  $Fd\bar{3}m$  structure result in an insulating CO solution which is compatible with the Verwey CO model.

An analysis of occupation matrices of  $3d$ -Fe<sub>B</sub> minority spin states confirms substantial charge disproportionation. As shown in Table I, one of the  $t_{2g\downarrow}$  states of Fe<sub>B(1)}</sub><sup>2+</sup> and Fe<sub>B(4)}</sub><sup>2+</sup> cations is almost completely filled with the occupation numbers  $n \approx 0.8$ . On the other hand, the remained two  $t_{2g\downarrow}$  orbitals of the Fe<sup>2+</sup> cations have significantly smaller population of about 0.15. The occu-

TABLE I: Total and  $l$ -projected charges, magnetic moments, and the occupation of the most populated  $t_{2g}$  minority orbital calculated for inequivalent  $Fe_B$  ions in the low-temperature  $P2/c$  phase of  $Fe_3O_4$  [28].

$Fe_B$ ion	$q$	$q_s$	$q_p$	$q_d$	$M$ ( $\mu_B$ )	$t_{2g\downarrow}$ orbital	$n$
$Fe_{B(1)}$	6.04	0.17	0.19	5.69	3.50	$d_{xz} \mp d_{yz}$	0.76
$Fe_{B(2)}$	5.73	0.19	0.21	5.44	3.94		0.27
$Fe_{B(3)}$	5.91	0.19	0.21	5.51	3.81		0.24
$Fe_{B(4)}$	6.03	0.16	0.18	5.69	3.48	$d_{x^2-y^2}$	0.80

pation numbers of  $t_{2g\downarrow}$  orbitals for  $Fe_{B(2)}^{3+}$  and  $Fe_{B(3)}^{3+}$  do not exceed 0.3, which gives the value of about 0.5 for the largest difference between  $Fe_B^{2+}$  and  $Fe_B^{3+}$   $t_{2g}$  minority spin populations. The corresponding total 3d charges difference (0.23) and disproportionation of the total electron charges inside the atomic spheres of  $Fe_B^{2+}$  and  $Fe_B^{3+}$  cations (0.24) is in a reasonably good agreement with the value of 0.2 estimated from BVS analysis of monoclinic structure. This shows that the change of the  $t_{2g\downarrow}$  occupations caused by the charge ordering is very effectively screened by the rearrangement of the other Fe electrons.

Significant contribution to the charge screening is provided by  $Fe_B$   $e_g$  states. Although the bands originating from these states are located well above the energy gap, the  $e_g$  minority orbitals form relatively strong  $\sigma$ -bonds with 2p-states of the oxygen octahedron and, as a result, give appreciable contribution to the occupied part of the valence band. The above mentioned screening reduces the energy loss due to the development of CO incompatible with the Anderson criterion in the LT phase of  $Fe_3O_4$ . Hence, due to strong screening effects, the order parameter, introduced as the total 3d charge difference between 2+ and 3+  $Fe_B$  cations, is ill-defined. That explains why the BVS analysis does not give convincing proof of CO existence. Apparently, the well-defined order parameter is the difference of  $t_{2g\downarrow}$  occupancies for  $Fe_B^{3+}$  and  $Fe_B^{2+}$  ions, which amounts to 50% of ideal ionic CO model and clearly pronounces the existence of CO below the Verwey transition.

The self-consistent solution obtained from the LSDA+U calculations is not only charge but also orbitally ordered. The occupied minority spin  $t_{2g}$  state of  $Fe_{B(1)}^{2+}$  and  $Fe_{B(4)}^{2+}$  cations is predominantly of  $d_{xz} \pm d_{yz}$  and  $d_{x^2-y^2}$  character, respectively. This is illustrated by Fig. 2 which shows the angular distribution of the minority spin 3d  $Fe_B$  electron density. Note, however, that the  $P2/c$  frame is rotated by an angle  $\sim \pi/4$  with respect to the cubic one and the angular dependence of  $t_{2g}$  states is given by  $d_{xy} \pm d_{yz}$  and  $d_{x^2-y^2}$  combination of cubic harmonics. The obtained relative orientation of occupied  $Fe_B$   $t_{2g}$  minority orbitals corresponds to the anti-ferro-orbital order. Since all  $Fe_B$  cations are ferromagnetically coupled, the obtained orbital order is consistent with the anti-ferro-orbital ferromagnetic state, which is

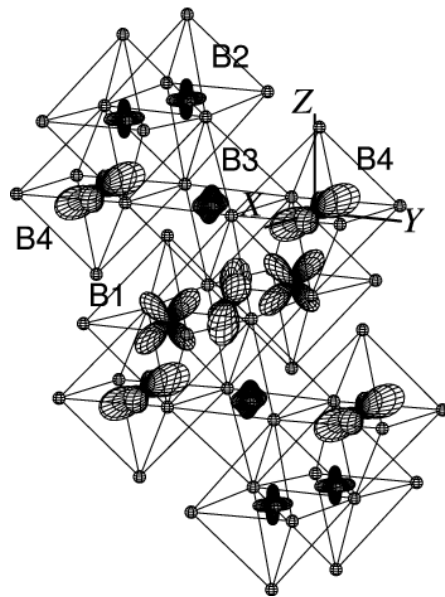


FIG. 2: The LSDA+U angular distribution of the minority spin 3d electron density of  $Fe_B$  cations for the low-temperature  $P2/c$  phase of  $Fe_3O_4$ . The angular distribution is calculated according to  $\rho(\theta, \phi) = \sum_{m, m'} n_{m, m'} Y_m^*(\theta, \phi) Y_{m'}(\theta, \phi)$ , where  $n_{m, m'}$  is the occupation matrix of  $d$  minority states for  $Fe_B$  atoms.  $Y_m(\theta, \phi)$  are corresponding spherical harmonics. Oxygen atoms are shown by small spheres. The size of orbital corresponds to its occupancy.

the ground state of the degenerate Hubbard model according to the Kugel-Khomskii theory [29]. This orbital order leads to the corresponding distortions of  $FeO_6$  octahedra. An analysis of interatomic distances in the monoclinic structure (Table II) shows that the average  $Fe_{B(1)}-O$  distance (2.087 Å) in the plane perpendicular to one of the diagonals of the distorted  $Fe_{B(1)}O_6$  octahedron is considerably larger than average distances in the other two planes (2.063 and 2.067 Å). It turns out that the occupied  $Fe_{B(1)}$   $t_{2g}$  minority spin orbital is the one oriented in the plane with the largest average  $Fe_{B(1)}-O$  distance. The same is also true for  $Fe_{B(4)}$  ion but in this case the variation of the average  $Fe_{B(4)}-O$  distances is smaller (2.074 Å vs.  $2 \times 2.067$  Å) and, as a consequence, the out-of-plane rotation of the occupied  $t_{2g\downarrow}$  orbital is stronger.

As was shown earlier, the Verwey CO model possesses the minimum electrostatic repulsion energy among all possible CO models [7]. But due to the existence of two perpendicular families of  $B$ -site chains (for instance  $[110]_c$  and  $[\bar{1}\bar{1}0]_c$ ) correspondingly occupied by 2+ and 3+  $Fe_B$  cations the lattice “feels” significant stresses and tends to expand in one ( $[110]_c$ ) and to compress in the another ( $[\bar{1}\bar{1}0]_c$ ) direction. Therefore, the Verwey CO gives a significant “elastic” energy contribution into the total energy and in spite of the lowest electrostatic energy

TABLE II: The averaged  $\text{Fe}_B\text{-O}$  distances in the plane of  $t_{2g}$  orbitals for  $P2/c$  structure of  $\text{Fe}_3\text{O}_4$  [28]

$\text{Fe}_B$ atom	orbital	$d_{\text{orb.}}$ ( $\text{\AA}$ )	$d_{\text{av.}}$ ( $\text{\AA}$ )
$\text{Fe}_{B(1a)}$	$d_{xz} + d_{yz}$	2.067	2.072
	$d_{xz} - d_{yz}$	2.087	
	$d_{x^2-y^2}$	2.063	
$\text{Fe}_{B(1b)}$	$d_{xz} + d_{yz}$	2.087	2.072
	$d_{xz} - d_{yz}$	2.067	
	$d_{x^2-y^2}$	2.063	
$\text{Fe}_{B(4)}$	$d_{xz} \pm d_{yz}$	2.067	2.069
	$d_{x^2-y^2}$	2.074	

becomes less favorable than other arrangements. The competition of these two (elastic and electrostatic) contributions in the total energy appears to be responsible for the charge order, which is realized in the experimentally observed low-temperature monoclinic structure. In this CO scheme the alternating  $(001)_c$  planes occupied by  $2+$  (“occupied” plane) and by  $3+$  (“empty” plane)  $\text{Fe}_B$  cations are separated by the “partially” occupied plane. This  $(001)_c$  planes order makes the difference between  $[110]_c$  and  $[\bar{1}\bar{1}0]_c$  directions less pronounced and significantly reduces the lattice stress and, as a result, reduces the elastic energy contribution in the total energy. We propose that this scenario is the primary cause for development of the class-I CO found below the Verwey transition.

In summary, in the present LSDA+ $U$  study of the LT  $P2/c$  phase of  $\text{Fe}_3\text{O}_4$  we found a charge and orbitally ordered insulator with an energy gap of 0.18 eV. This is in a good agreement with the experimental value of 0.14 eV [27]. The obtained charge ordered ground state is described by a dominant  $[001]_c$  charge density wave with a minor  $[00\frac{1}{2}]_c$  modulation. The CO coincides with the earlier proposed class-I CO [15, 16] and confirms a violation of the Anderson criterion [5]. While the screening of the charge disproportion is so effective that the total  $3d$  charge disproportion is rather small (0.23), the charge order is well pronounced with an order parameter defined as a difference of  $t_{2g\downarrow}$  occupancies of  $2+$  and  $3+$   $\text{Fe}_B$  cations (0.5). This agrees well with the result of BVS analysis for monoclinic structure (0.2). The orbital order is in agreement with the Kugel-Khomskii theory [29] and corresponds to the local distortions of oxygen octahedra surrounding  $\text{Fe}_B$ -sites.

We are grateful to D. Schrupp, R. Claessen, J. P. Attfield, P. Fulde, and D. Vollhardt for helpful discussions. The present work was supported by RFFI Grant No. 01-02-17063 and by DFG through Grant No. 484.

- [2] J. M. D. Coey, A. E. Berkowitz, L. Balcells, F. F. Putris, and F. T. Parker, Appl. Phys. Lett. **72**, 734 (1998).
- [3] E. J. W. Verwey, Nature (London) **144**, 327 (1939).
- [4] E. J. W. Verwey, P. W. Haayman, and F. C. Romeijan, J. Chem. Phys. **15**, 181 (1947).
- [5] P. W. Anderson, Phys. Rev. **102**, 1008 (1956).
- [6] M. Mizoguchi, J. Phys. Soc. Japan **44**, 1501 (1978).
- [7] J. M. Zuo, J. C. H. Spence, and W. Petuskey, Phys. Rev. B **42**, 8451 (1990).
- [8] M. Iizumi, T. F. Koetzle, G. Shirane, S. Chikazumi, M. Matsui, and S. Todo, Acta Cryst. **B38**, 2121 (1982).
- [9] Several reviews of research on the Verwey transition up to 1980 are contained in the special issue of Philos. Mag. B **42** (1980).
- [10] J. R. Cullen and E. R. Callen, Phys. Rev. Lett. **26**, 236 (1971).
- [11] J. R. Cullen and E. R. Callen, Phys. Rev. B **7**, 397 (1973).
- [12] N. F. Mott, Philos. Mag. B **42**, 327 (1980).
- [13] Y. Yamada, Philos. Mag. B **42**, 377 (1980).
- [14] H. Seo, M. Ogata, and H. Fukuyama, Phys. Rev. B **65**, 085107 (2002).
- [15] J. P. Wright, J. P. Attfield, and P. G. Radaelli, Phys. Rev. Lett. **87**, 266401 (2001).
- [16] J. P. Wright, J. P. Attfield, and P. G. Radaelli, Phys. Rev. B **66**, 214422 (2002).
- [17] Z. Szotek, W. M. Temmerman, A. Svane, L. Petit, G. M. Stocks, and H. Winter, Phys. Rev. B **68**, 054415 (2003).
- [18] V. I. Anisimov, J. Zaanen, and O. K. Andersen, Phys. Rev. B **44**, 943 (1991).
- [19] A. I. Liechtensten, V. I. Anisimov, and J. Zaanen, Phys. Rev. B **52**, 5467 (1995).
- [20] J. García, G. Subías, M. G. Proietti, J. Blasco, H. Renevier, J. L. Hodeau, and Y. Joly, Phys. Rev. B **63**, 054110 (2001).
- [21] J. García, G. Subías, J. Blasco, and M. G. Proietti, condmat/0211407 (2002).
- [22] J. García, G. Subías, M. G. Proietti, H. Renevier, Y. Joly, J. L. Hodeau, J. Blasco, M. C. Sánchez, and J. F. Béjar, Phys. Rev. Lett. **85**, 578 (2000).
- [23] V. N. Antonov, B. N. Harmon, V. P. Antrpov, A. Y. Perlov, and A. N. Yaresko, Phys. Rev. B **64**, 134410 (2001).
- [24] V. I. Anisimov, I. S. Elfimov, N. Hamada, and K. Terakura, Phys. Rev. B **54**, 4387 (1996).
- [25] Z. Zhang and S. Satpathy, Phys. Rev. B **44**, 13319 (1991).
- [26] A. Yanase and N. Hamada, J. Phys. Soc. Japan **68**, 1607 (1999).
- [27] S. K. Park, T. Ishikawa, and Y. Tokura, Phys. Rev. B **58**(7), 3717 (1998).
- [28] Here:  $d_{xz} - d_{yz}$ ,  $d_{xz} + d_{yz}$ , and  $d_{x^2-y^2}$  correspond to  $d_{xz}$ ,  $d_{yz}$ , and  $d_{xy}$  orbitals  $t_{2g}$  in the local frame connected to an oxygen octahedron or in the  $Fd\bar{3}m$  frame.
- [29] K. I. Kugel and D. I. Khomskii, Sov. Phys. Solid State **17**, 285 (1975).

[1] D. C. Mattis, *The Theory of Magnetism I* (Springer, Berlin 1988).